DEUTSCHES ELEKTRONEN-SYNCHROTRON DESY

DESY SR 86-13
December 1986

SOFT X-RAY SCATTERING FROM ROUGH SURFACES - EXPERIMENT AND THEORETICAL ANALYSIS

by

H. Hogrefe, C. Kunz

II. Inst. f. Experimentalphysik, Universität Hamburg

and

Hamburger Synchrotronstrahlungslabor HASYLAB at DESY

ISSN 0723-7979

NOTKESTRASSE 85 · 2 HAMBURG 52

To be sure that your preprints are promptly included in the
HIGH ENERGY PHYSICS INDEX ,
send them to the following address (if possible by air mail) :

DESY
Bibliothek
Notkestrasse 85
2 Hamburg 52
Germany

DESY SR 86-13
December 1986

ISSN 0723-7979

Soft X-Ray Scattering from Rough Surfaces - Experiment and Theoretical Analysis

H. Hogrefe* and C. Kunz

Universität Hamburg, II. Institut f. Experimentalphysik

Luruper Chaussee 149, D-2000 Hamburg 50, F.R. Germany

and

HASYLAB, DESY, Notkestr. 85, D-2000 Hamburg 52, F.R. Germany

Specularly reflected and scattered radiation was measured at λ = 50, 100, 200 Å from artificially roughened flat mirrors and from thick vacuum evaporated Au samples. The results of the roughened samples are in reasonable agreement with Beckmann's scalar theory using an exponential autocorrelation function. The angle dependent scattering distributions at different angles of incidence and different wavelengths are described with a unique mean roughness and autocorrelation length. The application of the vector theory in its simplest analytical form is not successful, however, it provides a means to qualitatively correct the scalar theory for the influence of the actual optical constants of the scattering surface in agreement with experiments. The thick Au films are roughened due to surface crystallization and yield completely different scattering distributions. These results could not be fitted with scalar theory neither with an exponential nor with a gaussian autocorrelation function.

---

submitted to Appl. Opt.

* now with: University of California, Lawrence Berkeley Laboratory, Center for X-ray Optics, Berkeley, CA 94720, USA

1. Introduction

A proper understanding of surface scattering in the vacuum ultraviolet (VUV) and soft x-ray regions becomes increasingly important as these spectral regions are now quite readily accessible due to the availability of intense synchrotron radiation. Valuable information on surface topology can be obtained in principle from surface scattering experiments. This involves a theoretical analysis of the scattering data. The applicability of several commonly used theoretical approximations needs to be tested. Not less important aims are the study of the influence of preparation methods on the surface structure of thin films, crystals, optical surfaces etc. and the standard evaluation of the performance of optical elements for example of mirrors for soft x-ray telescopes used in space astronomy.

Investigations of this kind have been widely performed with lasers in the visible or with hard x-ray line sources (see e.g. /1-8/) since these supply the necessary intensity in a well collimated beam. In the VUV- or soft x-ray wavelength range (λ = 20 - 1000 Å) only a few investigations have been carried out on light scattering /9,10/. Our interest in the optical properties of solids at these wavelengths and the availability of the synchrotron radiation source DORIS II led us to a broader investigation of this subject.

The overlap between scattering results applying different wavelengths (and also those of other surface inspection methods like the use of stylus instruments) is limited since each method emphasizes a special range of vertical and horizontal surface structures /11/. The major reason is explained from the simple grating equation, decomposing the roughness into Fourier components

corresponding to sinusoidal gratings. Then it is easily seen that it is impossible to resolve grating spacings less than $\lambda/2$ (Rayleigh limit). Another limitation arises for short wavelengths mainly for x-ray scattering from the lower reflectivity in this spectral range which allows only scattering at very grazing angles of incidence and only near the direction of specular reflection. Combining these two aspects we conclude that scattering of soft x-rays (typically at λ = 100 Å and 80° angle of incidence) will mainly be determined by lateral spacings in the order of 100 Å - 1 µm. This region is not accessible by visible light because of the Rayleigh limit and also not easily accessible by x-rays because of intensity reasons. In addition, the experimental conditions, such as the detector apertures set further limits.

In this paper we restrict our analysis to theories which deal with a single surface that can be statistically described in terms of the isotropic autocorrelation function C /12,13/ and which yield results in closed analytic form. Following Kirchhoff's method Beckmann /13/ has developed a well-known scalar theory based on several assumptions of which the most important are 1) the roughness curvature radii have to be large compared to the wavelength ("tangent plane approximation") and 2) the neglect of the influence of the optical constants (reflectivity R_0 = 1) on the scattering distribution. Among the various methods taking into account the vector character of the electromagnetic wave and thereby optical constants and polarization, we consider here the perturbation theory developed among others by Elson /14/ and Church /11/, which has the single limitation that the rms-roughness σ has to be small: $\sigma \ll \lambda$.

Both theories are described in section II. Each of them has advantages and disadvantages. The final equations are similarly structured arithmetic expressions containing two separate terms for the specular and diffusely reflected intensity.

The roughness induced reduction of the specular reflectivity which is related to the so-called Total Integrated Scatter TIS, is at least for lateraly large structures /15/ mainly influenced by the rms-roughness σ while the distribution of the intensity scattered into different elements of solid angle is mostly governed by the autocorrelation length T, a measure for the mean lateral separation and/or extension of the surface structures.

In section III, we concentrate on the T-dependence of the scattering distribution for various angles of incidence and various VUV-wavelengths. For this purpose, and especially to prove the sensitivity of light in our spectral region to structures with short spacial frequencies we prepared two different kinds of rough samples, a) by polishing glass substrates with polish of different grain size and evaporating thereafter thin overlayers of gold and b) by evaporating thick layers of gold, which are known to form rough surfaces due to the growth process. We expected to get samples with the same mean roughness amplitude but with different autocorrelation lengths T. Also scattering distributions of uncoated polished substrates with nearly the same surface topology were obtained in order to investigate the influence of the optical constants and thereby the suitability of the theories. Because of this intentional roughening our samples are rougher than state of the art optical surfaces. On the other hand the altogether weak signal of scattered light becomes measurable with good accuracy and therefore a comparison with theory is meaningful. The results are summarized in section IV.

II. Theory

The scattering geometry is easily explained (see fig. 1): An electromagnetic wave with a wavelength λ (wavevector $|\vec{k}| = \frac{2\pi}{\lambda}$) is incident on a moderately rough surface at an angle θ_1 to the surface normal and is scattered at the polar scattering angle θ_2 and the azimuthal angle θ_3. The specular direction is then described by $\theta_1 = \theta_2$ and $\theta_3 = 0$. Since our measurements have been always carried out in the plane of incidence, θ_3 will be zero throughout this paper.

As mentioned already in the introduction and also by other authors, e.g. /11/, basic properties of the scattered light can be roughly derived from very simple considerations:

1. The phase difference $\Delta\varphi$ which two neighbouring rays undergo when they are reflected specularly from different levels on the surface, where h is the height difference (fig. 2), is given by the following relation:

$$\Delta\varphi = \frac{4\pi}{\lambda} \cdot h \cdot \cos\theta_1$$

This $\Delta\varphi$, if small, should be related to the loss of intensity in the specular direction. For reasons of energy conservation the loss in specularly reflected intensity should be related to the total scattered intensity TIS (Total Integrated Scatter), although a possible additional surface absorption is neglected in this consideration. We conclude that the TIS is a monotonously

rising function of $\sigma/\lambda \cos\theta_1$, where σ is the mean roughness.

2. The grating equation must hold for each single Fourier component of the rough surface:

$$\sin\theta_2 = \sin\theta_1 + m\frac{\lambda}{d} \qquad m = \pm 1, \pm 2, \ldots$$

$$d = \text{"grating" constant}$$

From this we learn, that the spread of the scattered intensity over the different angles θ_2 is dependent on d, such that the scattering distribution becomes broader if d becomes smaller (or if the incident intensity is more grazing). The angular distribution of the scattered intensity $I(\theta_2)$ will be a function of λ/d and $\sin\theta_1$.

All this has of course to be confirmed by a rigorous theoretical treatment. In order to arrive at that goal, we first have to specify the nature of the rough surface /13/. The coordinates of the surface shall be $\vec{r} = (x,y,z = \xi(x,y))$ where $\xi(x,y)$ represents the rough surface with the mean surface level at $z = 0$.

The theories which are outlined here, consider the surface height to be a random variable which is fully characterized by a two-dimensional probability distribution $p(z_1,z_2)$ giving the probability that the surface heights $\xi(x,y)$ at two different lateraly separated points 1 and 2 assume values z_1 and z_2. This distribution is mostly assumed to be isotropic and gaussian with respect to the surface heights. It can then be represented by its variance $\langle\xi^2\rangle$ and the autocorrelation function $C(\tau) = \langle\xi(\vec{r})\ \xi(\vec{r}+\vec{\tau})\rangle/\langle\xi^2\rangle$ with the

separation parameter $\tau = |\vec{r}_2 - \vec{r}_1|$. The variance is equal to the square of the rms-roughness, so that it gives us an information about the roughness depth, while the autocorrelation function characterizes the lateral surface statistics. For two very close points correlation should be perfect, $C(0) = 1$, while $C(\tau)$ usually decreases rapidly for randomly rough surfaces with increasing separation τ. The value $\tau = T$, for which $C(T) = 1/e$, is called the autocorrelation length and provides a measure for the mean lateral size of the surface structures. $\sqrt{\langle \xi^2 \rangle} = \sigma$ and $C(\tau)$ (or T) allow a practical description of the surface, which is needed for ensemble averaging in the scattering theories. $C(\tau)$ can well be constructed from several surface height measurements with a profilometer /12/. Such measurements are of course bandwidth limited, e.g. most optical and mechanical stylus profilometers are restricted to lateral separations $\gtrsim 1$ µm. $C(\tau)$ is often given in an analytical form, mostly as exponential or gaussian:

$$C_e = e^{-|\tau|/T} \qquad \text{or} \qquad C_g = e^{-\tau^2/T^2}$$

For real surfaces these are good approximations at best.

The scalar scattering theory /13/ is similar to Kirchhoff's treatment of the diffraction of an electromagnetic wave E by a plane screen with a hole /16/. The vector character of the field is neglected. Starting with Helmholtz's integral, which relates the scattered field at the far zone observation point to the total field $(E)_{surface}$ on the rough surface, one has to make proper assumptions about the boundary conditions $(E)_{surface}$ and $(\delta E/\delta n)_{surface}$. This is done by expressing the field in terms of the Fresnel reflection coefficient $R_o = |\hat{r}|^2$ for a tangent plane at each point of the surface,

which can be done reasonably only when the rough surface is changing its slope slowly at distances comparable to the wavelength λ ("tangent plane approximation"). Even with this approximation the Helmholtz integral cannot simply be evaluated since one does not know the reflectivity R_o(local angle of incidence) at each microscopic point on the surface. For this reason Beckmann assumes infinite conductivity to make $R_o = 1$ or takes an average reflectivity $R_o(\theta_1)$, neglecting the local reflectivity variations at each integration point. Finally, to obtain the scattered intensity per solid angle element one has to perform ensemble averaging of the integrals which involves the above statistical description of the surface. Gaussian height distribution and a particular autocorrelation function result in the following final expression:

$$\frac{dI}{I_o d\Omega} = R_o(\theta_1)\, e^{-g}\, \delta(\theta_1 - \theta_2) + R_o(\theta_1)\, e^{-g}\, \frac{1}{\lambda^2}\, F(\theta_{1,2,3}) \sum_{m=1}^{\infty} \frac{g^m}{m!}\, W_m \qquad (1)$$

$$= I_{specular} + I_{scatter}$$

with

$$g = \frac{4\pi^2\sigma^2}{\lambda^2}\,(\cos\theta_1 + \cos\theta_2)^2$$

g determines the convergence of the series in $I_{scatter}$,

and

$$F(\theta_{1,2,3}) = \frac{(1 + \cos\theta_1\cos\theta_2 - \sin\theta_1\sin\theta_2\cos\theta_3)^2}{\cos\theta_1\,(\cos\theta_1 + \cos\theta_2)^2}$$

W_m assumes the following expressions for exponential and gaussian autocorrelation functions $C(\tau)$:

$$W_{m,e} = \frac{2\pi(1/m)^2}{(1 + (1/m)^2 V_{xy}^2)^{3/2}} \quad \text{or} \quad W_{m,g} = \frac{\pi}{m} l^2 e^{-V_{xy}^2 l^2/4m}$$

where

$$V_{xy}^2 = |\bar{k}_1 - \bar{k}_2|^2 = (\sin^2\theta_1 - 2\sin\theta_1 \sin\theta_2 \cos\theta_3 + \sin^2\theta_2)\frac{4\pi^2}{\lambda^2}$$

The first term turns out to be the well-known expression $R_o \exp[-(4\pi\sigma\cos\theta_1/\lambda)^2]$ which differs from zero only for $\theta_2 \approx \theta_1$ (indicated by the δ-function) yielding a reduced specular reflectivity $R(\theta_1)$ (it is assumed that the light incident on the sample is a parallel wave). The scattering distribution $I_{scatter}$ mainly contains a geometry factor F ("obliquity factor"), a power series containing the surface statistics in terms of W_m and a λ-dependent factor. The further factor $R_o(\theta_1)$ is the only one in which the scalar theory includes the optical constants of the material correcting only the $\theta_2 = \theta_1$-direction of the $I_{scatter}$-distribution to the proper reflectivity. For very small roughnesses σ ($g \ll 1$) higher order terms of the series can be neglected. Then $I_{scatter}$ is proportional to W_1, which is the so-called power spectral density function (PSD) and can be regarded as the Fourier transform of the roughness. There is some uncertainty in the literature about the exact form of the geometry factor F (compare /2,3,6,13/). We took the one also Aschenbach et al. used /6/ without applying their grazing incidence approximations. As a check we numerically integrated the whole $dI/(I_o d\Omega)$-distribution for different angles θ_1, over the full solid angle Ω and always obtained unity (for $R_o = 1$) as expected, which could not be achieved for the other proposed F-factors.

The above result of Beckmann's theory proves our previous conclusions 1 and 2: $I_{specular}$ and consequently the TIS is only dependent on $\sigma/\lambda \cdot \cos\theta_1$.

The scattering distribution $I_{scatter}$ still contains both σ (in g) and T (in W) but for grazing incidence their influence can be separated. σ determines only the scattering intensity level and T the distribution shape. In order to show this, we have computed equation (1) for an exponential autocorrelation function applying realistic parameters σ and T which are accessible to our reflectometer. Figure 3 shows that the distributions behave as expected. Only, when g becomes large (i.e. $\theta_1 < 75°$, $\sigma/\lambda > 0.5$) σ has some influence also on the shape of the distributions.

We are now turning to the vector scattering theory. In its form which we use here for comparative purposes /14/ is based on the first order perturbation solution of the Helmholtz differential equation which shall not be dealt with in detail here. Since the vector character of the electromagnetic field is not neglected the incident, transmitted, and reflected light may be polarized and furtheron reflectivities $R_o \neq 1$ are treated more correctly. There is no restriction on the shape of the roughness as it is the case with the scalar theory. The only restriction is $\sigma \ll \lambda$ because of the first order perturbation treatment. This is of course a severe limitation for soft x-ray wavelengths.

It happens that the result of this theory is quite similar to (1):

$$\frac{dI}{I_o d\Omega} = I_{specular} + \frac{16\pi^2}{\lambda^4} F(\theta_{1,2})\ \sigma^2 \cdot Q \cdot W_1 \qquad (2)$$

with $F(\theta_{1,2}) = \cos\theta_1 \cos^2\theta_2$

and the factor Q for s-polarized incident radiation and $\theta_3 = 0$:

$$Q = |\hat{\varepsilon}-1|^2 \left| \frac{1}{\cos\theta_1 + \sqrt{\hat{\varepsilon}-\sin^2\theta_1}\,(\cos\theta_2 + \sqrt{\hat{\varepsilon}-\sin^2\theta_2})} \right|^2$$

Again, the scattered intensity distribution is dominated by the power spectral density (PSD)-function, a geometry factor ($F(\theta_{1,2})$) and a factor Q replacing $R_0(\theta)$ and containing the optical constants ($\hat{\varepsilon}$) and polarization properties. Indeed, it turns out, that in the limit of $\sigma \ll \lambda$, $\theta_2 = \theta_1$, Q equals R_0 and both theories provide an identical expression. For the specularly reflected intensity $I_{specular}$ we take the same form as in eq. (1).

In figure 4 scattering distributions $I_{scatter}$ calculated with eqs. (1) and (2) using the exponential autocorrelation function are compared for $\theta_1 = 80°$, $\lambda = 100$ Å and $\sigma = 30$ Å. Vector theory (Q = 1) and scalar theory differ only for large values of $\theta_2 - \theta_1$ (away from the specular direction). This is due to the contribution of the higher order terms in eq. (1) and to the different geometry factors. The other curves show the influence of the reflectivity $R_0 \neq 1$ for glass, the substrate we used, and gold. Basically $R_0 \neq 1$ results in a decrease of the scattered intensity for $\theta_2 < \theta_1$ and in an increase for $\theta_2 > \theta_1$ compared to the $R_0 = 1$ case.

For materials which have a steep reflectivity decrease at the cut-off angle this decrease should also be found in the scattering distribution since Q is structured similarly to the Fresnel equations.

In summarizing we may state that the vector theory should be preferred for small roughnesses because of its more general approach including especially the "optical factor" Q. The advantage of the scalar theory is that it is able to take into account larger roughnesses as long as σ is not larger

than the wavelength. But this may be of crucial importance for soft x-rays if the investigated surface is not extremely smooth.

III. Experimental results and discussion

The experiments discussed here were carried out with the VUV-reflectometer /17/ of the Hamburg Synchrotron Radiation Facility (HASYLAB) at DESY. This instrument is capable of the high precision rotations and translations required for accurate scattering and reflectivity measurements. All measurements were made with s-polarized light and the scattering distributions were determined only in the plane of incidence. The instrument is capable in principle also to measure off-plane straylight and in situ prepared samples under ultrahigh vacuum conditions. With some modifications also measurements with light incident in p-polarization are feasible but this option was not used in this investigation.

Two different types of detectors were used for these measurements. For accurate absolute measurements a photodiode coated with Al_2O_3 connected to a DC amplifier was used. An open photomultiplier equipped with a KCl coated cathode was used to obtain angular distributions with good angular resolution and whenever it was necessary to follow the tails of the scattering distribution to very low intensity levels.

The samples were prepared by evaporation of gold films with different thicknesses onto a smooth or roughened glass substrate. The currently available dynamical range of our signal electronics forced us to do most of the investigation with artificially roughened samples. This enabled us to produce different

types and degrees of roughnesses. Unfortunately at the time when the experiments were performed, the evaporation in the reflectometer was not possible yet, so that the samples had contact with air before being measured.

One series of samples was prepared by coating glass substrates which were polished with 1 µm or 15 µm diamond grains (in order to roughen them) with 500 Å gold. As our minimum coating thickness 500 Å was chosen in order to avoid interference effects within the thin films. The thin 500 Å gold coating should reproduce the substrate roughness but not introduce any appreciable roughness of its own, so that the stray light mainly arises from polishing. To confirm the reproduction of the surface structure by the coating and to investigate the influence of the optical constants of the two materials on the scattered light we also measured in several cases (see below) the uncoated but roughened substrate.

The second type of samples was then produced by evaporation of 500 Å, 1000 Å, and 2000 Å gold onto smooth glass substrates ($\sigma \approx 5$ Å). With increasing coating thickness the roughness of Au increases and the scattering properties finally are dominated by the structures of the gold film. Consequently the 500 Å film on a not re-polished substrate is the smoothest sample presented here. Since the lateral irregularities of evaporated thin films are typically of the size of the film thickness, we expect the lateral dimensions of the roughness of the thick Au films to be smaller than those of the polished samples.

The dotted curves in figs. 5-9, 11 show the experimentally determined scattering distributions $\log \left(\frac{1}{R_o(\Theta_1) I_o} \frac{dI}{d\Omega}\right)$ for 6 samples including the specular reflected peaks and the incident intensity profile I_o (not shown in all figures). Because of serious difficulties not all samples have been measured over the same variety of parameters (Θ_1, λ). The curves were normalized with respect to I_o, the incident intensity, and each distribution was divided by its corresponding Fresnel reflectivity R_o at Θ_1 /18,19/ so that the lowering of the peaks with increasing grazing angle is a direct measure for σ and represents the factor $\exp\left[-(4\pi\sigma \cos\Theta_1/\lambda)^2\right]$ of eq. (1). $I_{scatter}$ can be separated very well from $I_{specular}$ by comparing the angular distributions with that of I_o. All curves exhibit a pronounced dependence on the wavelength and angle of incidence resulting in changes of the scattering distributions and their intensity level with respect to I_o and $I(\Theta_2=\Theta_1)$ (the peak intensities of each curve). Further scattering distributions are given in refs. /20,21/.

Already a first inspection of the experimental curves confirms some general trends predicted by the considerations 1. and 2. in section II as well as trends given by eqs. (1) and (2) of the previous chapter: e.g., fig. 6 shows very well that the scattered intensity level increases with decreasing wavelength and with decreasing angle of incidence Θ_1 (see especially the ratio $I_{specular}/I_{scatter}$ $(\Theta_2 = \Theta_1)$ of the experimental curves). Additionally, the distribution becomes broader with increasing wavelength and increasing Θ_1 just as predicted by the grating analogy. But there are as well some features of the scattering branches which are not so obvious to understand e.g. the changes in relative intensity at $\Theta_2 > \Theta_1$ to that at $\Theta_2 < \Theta_1$.

Comparing our results to the scattering theories of section II we obtain best results with the scalar theory of Beckmann. In making these fits we

used the fact that the shapes of the distributions are almost independent of the rms-roughness σ as we stated in section II. σ was determined from continous measurements of the specular reflectivity versus Θ_1 (not shown here) using the first term of eq. (1). With these σ-values for the different samples the fits were performed by varying mainly the autocorrelation length T and the ratio $I_{specular}$ to $I_{scatter}$. The latter is determined by the finite detector aperture Ω_d which was small compared to the broad scattering distribution. Since Ω_d, the solid angle subtended by the effective area on the photocathode, is difficult to measure accurately it was used as the fit parameter. Fits were made using Beckmann's scalar theory (eq. (1)) with an exponential autocorrelation function $C_e(\tau)$. The fits are shown as solid curves in figs. 5-8. The best fits were obtained for the polished samples (figs. 6 and 7), especially for the one polished with 1 µm-diamond paste. In the latter case it was possible to perform a very good fit with one parameter-set σ, T, Ω_d for all curves in fig. 6, and with Ω_d 70 % smaller than the solid angle determined from the geometrical detector aperture. Also the increase of the scattering intensity with decreasing Θ_1 is explained accurately by eq. (1) for this sample.

For the other samples Ω_d had to be adjusted differently for each particular distribution within a factor 3. For the smooth "500 Å-sample" and the "15 µm-polished" sample the scalar theory still gives consistent information about the autocorrelation length T.

The results of all fits with eq. (1) are summarized in table 1. The thick gold films yielded only a reasonable fit for the 1000 Å thick films (not shown here, see refs. /20,21/) for $\Theta_1 = 80°$; in the case of the 2000 Å film

(fig. 8) no really satisfactory fit could be achieved. These samples give totally different scattering patterns than the other samples. The deduced T-values can therefore only be understood as rough estimates. Nonetheless, they are confirming our expectation that the gold film roughness yield lateral structures with smaller sizes than the polishing process.

We also tried to make the fits with a gaussian autocorrelation function $C_g(\tau)$ but the upper part of fig. 9 demonstrates for one sample that the general shape of the curves evaluated from eq. (1) with $C_g(\tau)$ is not able to explain any of the experimental scattering distributions. This is in agreement with the experience of other authors, who preferred exponential autocorrelation functions to explain visible light- or x-ray measurements /7,22/.

Some features of the measurements, however, remain unexplained from eq. (1) using $C_e(\tau)$. The main discrepancy is the high scattering intensity (shoulder) in the right branch of all distributions measured for $\Theta_1 = 70°$ and $\lambda = 100$ Å. This effect appears to be even somewhat increased for larger roughnesses σ.

In section II it was mentioned that Beckmann's theory does not include the effect of the finite reflectivity $R_0 \neq 1$ on the scattering distribution so that the theoretical curves of figs. 5-8 have to be modulated by an optical factor. For Elson's vector theory such an optical factor (Q) is available. Since both theories have similar structure of the final analytical results we consider here only the possible improvement by applying the vector theory (using $C_e(\tau)$) for the "1 µm-polished" sample which was so well explained by the scalar theory (see fig. 6).

The lower part of fig. 9 shown the vector theory calculated for the parameters σ, T, Ω_d already deduced from scalar theory. From this fit it is obvious that the 1. order vector theory is not able to give a better fit to the experimental curves than the scalar theory. An attempt to improve the fit by varying T gave the result that we had to reduce T from 2500 Å (see table 1) to roughly T = 800 Å to get a better fit for λ = 100 Å. At λ = 200 Å, however, the agreement which was better there before disappeared. We suggest that our samples are too rough to fulfil the necessary condition $\sigma \ll \lambda$ for using the vector theory in the form of eq. (2). This equation is just lacking the additional terms W_m ($m > 1$) which are included in eq. (1).

Nonetheless the optical factor Q of eq. (2) can give us a hint in which direction the theoretical curves based on the scalar theory may have to be corrected. $Q(\Theta_2)$ has a similar shape as R_o as a function of Θ_1 (see fig. 10). Consequently the scalar curves should be lowered at the left branch and raised at the right branch to take into account the effect of the optical constants for the non-specular directions as required by the 1. order vector theory. This can be seen in the theoretical curves of fig. 4 for gold and glass. to prove this, we have measured also uncoated glass substrates which were prepared in the same way as our gold coated polished samples of figs. 6 and 7 so that the main difference in the scattering process should be the different Q-factors determined by the optical constants. Comparing both scattering distributions of fig. 11 clearly shows that the predicted lowering and raising of the branches really occurs. The amount of this effect is different for different samples (roughnesses), an observation which is not predicted by the 1. order Q-factor.

The drop in reflectivity near the critical angle, which occurs for gold at $\Theta_1 \approx 72°$ (λ = 100 Å), is also contained in Q as a function of Θ_2, i.e. there is also a similar drop in Q below $\Theta_2 \approx 72°$ (see fig. 10). We observe this as an especially pronounced change in slope between the left and right wings of our 70°-scattering distributions leading even to a shoulder in the scattering distribution of the thick Au film in fig. 8. At λ = 200 Å the Q-factor for gold does not show such a steep decrease but rather a slight continuous decrease from $\Theta_2 = 90°$ to $\Theta_2 = 50°$. And indeed the experimental curves at 200 Å do not exhibit that shoulder.

Thus, the Q-factor gives a qualitative understanding of some of the discrepancies between the scalar theory and the experimental curves. The fact that no consistent Q-factor corrected fit for all measurements of one sample could be found is probably due to the fact that the important condition $\sigma \ll \lambda$, for which the given Q is derived, is not valid.

Our experimental results are in agreement with x-ray scattering measurements of Yoneda /23/ and others /24,25/. These authors also measured a shoulder or even a peak at a fixed angle Θ_2 near the critical angle Θ_c ("Yoneda effect"). This effect only occurs when Θ_1 is smaller than Θ_c and is roughness dependent as in our case. Warren and Clarkes /24/ assumed a kind of "dirt layer" to explain the Yoneda-effect. This appears not to be the complete truth since the effect occurs also at reasonably clean surfaces as Guentert /25/ and we have shown. But to all these authors the Yoneda-effect appears to be related to the critical angle of total reflection. If the interpretation of the scattering measurements in terms of Q is correct, there should be changes in the wings of the distributions for all angles of incidence Θ_1

and not only for $\theta_1 < \theta_c$. Using an appropriate Q-factor, or better a higher order vector theory, which is not available yet, the whole scattering pattern should become explainable in terms of W_m, F and Q.

Conclusion

We have demonstrated experimentally, that soft x-ray surface scattering is a valuable method for the characterization of surface roughness in a region of lateral Fourier components in the order of 100 Å to 1 µm. We were able to obtain the results by using a new high-accuracy reflectometer using different photon energies and different angles of incidence. The measurements covered an intensity range of up to six orders of magnitude. Two kinds of surfaces with completely different angular distributions of the scattered radiation were investigated, namely artifically roughened samples by polishing with intermediate grain polish and thick evaporated gold films which are rough due to the re-crystallization during film growth.

We have analyzed our results with Beckmann's scalar scattering theory which on the one hand ignores the optical constants of the surface material but on the other hand is not limited to roughnesses with $\sigma \ll \lambda$. This theory yielded a good description of the results on the roughened samples with an exponential correlation function. The dependencies on angle of incidence and on wavelength were correctly reproduced. All spectra could be fitted reasonably well with one set of values for the mean roughness σ and the autocorrelation length T.

The vector theory after Elson did not allow to fit the data properly. This is understandable since it requires $\sigma \ll \lambda$ which probably is not fulfilled for our samples. From a comparison of the two theories and their similar structure a factor Q containing the dependencies on the optical constants is separable. This factor at least qualitatively explained the large asymmetry of the scattered radiation relative to the specularly reflected beam which was not reproduced by the scalar theory.

The roughness structure of thick Au films appears to be quite different. The scattering curves could not be reproduced with the scalar theory neither with an exponential correlation function nor with a gaussian correlation function. While the different character of the surface structures on polished samples and on thick vapour deposited Au films is immediately obvious from the shape of the angular distributions of scattered light, a better theory should enable us to extract further information on such surfaces from scattering data.

ACKNOWLEDGEMENT

We are indepted to R.-P. Haelbich for his collaboration in the early stage of this project and for many fruitful discussions. Likewise W. Jark has helped us with experimental support and by providing computer software. We are grateful to H. Zeiger for his careful preparation of the gold coatings of the samples. Likewise we thank S. Weigert for helping us by preparing the manuscript with great care. The work was supported under contract number 05 248 KU and 05 305 AX B/5 by the Bundesministerium für Forschung und Technologie. One of us (H.H.) acknowledges the support by the Office of Basic Energy Sciences, U.S. Department of Energy, under contract no. DE-AC03-765F00098.

References

/1/ R. Blazey, "Light scattering by laser mirrors", Appl. Opt. 6, 831 (1967).

/2/ R.J. Noll, P. Glenn, "Mirror and surface autocovariance functions and their associated visible scattering", Appl. Opt. 21, 1824 (1982).

/3/ Y. Wang, W.L. Wolfe, "Scattering from microrough surfaces: comparison of theory and experiment", J. Opt. Soc. Am. 73, 1596 (1983).

/4/ J.M. Benett, J.M. Elson, J.P. Rahn, "Angle-resolved scattering: comparison of theory and experiment, Proc. of the SPIE 401, 234 (1983).

/5/ P.A.J. de Korte, R. Lainé, "Assessment of surface roughness by x-ray scattering and differential interference contrast microscopy", Appl. Opt. 18, 236 (1979).

/6/ B. Aschenbach, H. Bräuninger, G. Hasinger, J. Trümper, "Measurements of X-ray scattering from Wolter type telescopes and various flat Zerodur mirrors", Proc. of the SPIE 257, 223 (1980).
B. Aschenbach, H. Bräuninger, A. Ondrusch, P. Predehl, "X-ray scattering of superpolished flat mirror samples", Proc. of the SPIE 316, 187 (1981).

/7/ R. Lenzen, "Abbildungseigenschaften eines Röntgenteleskops vom Typ Wolter-I unter besonderer Berücksichtigung der Kontrastminderung durch diffuse Reflexion", thesis, MPI f. Physik und Astrophysik, MPI-PAE/ Extraterr. 145, Sept. 1978.

/8/ T. Matsushita, I. Ishikawa, K. Kohra, "High-resolution measurements of angle-resolved X-ray scattering from optically flat mirrors", J. Appl. Cryst. 17, 257 (1984).

/9/ V. Rehn, V.O. Jones, J.M. Elson, J.M. Bennett, "The role of surface topography in predicting scattering at grazing incidence from optical surfaces", Nucl. Instr. and Meth. 172, 307 (1980).

/10/ J.M. Elson, V. Rehn, J.M. Bennett, V.O. Jones, "Measurement of angle resolved light scattering from optical surfaces in the 75-750 eV range", Proc. of the SPIE 315, 193 (1981).

/11/ E.L. Church, H.A. Jenkinson, J.M. Zavada, "Measurement of the finish of diamond-turned metal surfaces by differential light scattering", Opt. Eng. 16, 360 (1977).
E.L. Church, "Role of surface topography in X-ray scattering", Proc. of the SPIE 184, 196 (1979).
E.L. Church, H.A. Jenkinson, J.M. Zavada, "Relationship between surface scattering and microtopographic features", Opt. Eng. 18, 125 (1979).

/12/ J.M. Elson, J.M. Bennett, "Relation between the angular dependence of scattering and the statistical properties of optical surfaces", J. Opt. Soc. Am. 69, 31 (1979).

/13/ P. Beckmann, A. Spizzichino, "The scattering of electromagnetic waves from rough surfaces" (Pergamon, New York 1963).

/14/ J.M. Elson, "Light scattering from semi-infinite media for non-normal incidence", Phys. Rev. B12, 2541 (1975).
J.M. Elson, J.M. Benett, "Vector scattering theory", Opt. Eng. 18, 116 (1979).

/15/ J.M. Elson, J.P. Rahn, J.M. Bennett, "Relationship of the total integrated scattering from multilayer-coated optics to angle of incidence, polarization, correlation length, and roughness cross-correlation properties", Appl. Opt. 22, 3207 (1983).

/16/ M. Born, E. Wolf, "Principles of Optics", (Pergamon Press, New York 1975).

/17/ H. Hogrefe, D. Giesenberg, R.-P. Haelbich, C. Kunz, "A new reflectometer for UHV-applications", Nucl. Instr. and Meth. 208, 415 (1983).

/18/ H.-J. Hagemann, W. Gudat, C. Kunz, "Optical constants from the far infrared to the X-ray region: Mg, Al, Cu, Ag, Au, Bi, C, and Al_2O_3", DESY Report SR-74/7 (1974), and J. Opt. Soc. Am. 65, 742 (1975).

/19/ P. Sladeczek, "Bestimmung optischer Konstanten aus Reflektivitätsmessungen im VUV durch Vielwinkelanalyse und Kramers-Kronig-Analyse am Beispiel dünner Gold-Filme", Diplomarbeit, Universität Hamburg, 1985.

/20/ H. Hogrefe, R.-P. Haelbich, C. Kunz, "Specular and diffuse reflection of soft X-rays from mirrors", Nucl. Instr. and Meth. A246, 198 (1986).

/21/ H. Hogrefe, "Spekulare und diffuse Reflexion von weicher Röntgenstrahlung an optischen Oberflächen", thesis, Universität Hamburg, 1985, DESY-HASYLAB Report 85-05, 1985.

/22/ J. Eastman, P. Baumeister, "The microstructure of polished optical surfaces", Optics Commun. 12, 418 (1974).

/23/ Y. Yoneda, "Anomalous surface reflection of X-rays", Phys. Rev. 131, 2010 (1963).

/24/ B.E. Warren, J.S. Clarke, "Interpretation of the anomalous surface reflection of x-rays", J. Appl. Phys. 36, 324 (1965).

/25/ O.J. Guentert, "Study of the anomalous surface reflection of x-rays", J. Appl. Phys. 36, 1361 (1965).

Table 1 Roughness parameters for the different samples as determined.

sample	σ(Å) $\pm$ 3 Å	l (Å) $\pm$ 300 Å
polished glass (1 µm) (+ 500 Å Au)	27	2500
polished glass (15 µm) (+ 500 Å Au)	28	2000
500 Å Au on glass	18	1900
1000 Å Au on glass	29	700
2000 Å Au on glass	(43)	(1450)

Figure Captions

Fig. 1 The scattering geometry.

Fig. 2 Illustration of the phase difference $\Delta\varphi$ of neighbouring rays in the specular direction ($\Theta_2 = \Theta_1$), when they are reflected at different surface levels due to a roughness step h.

Fig. 3 The influence of the rms-roughness σ and the autocorrelation length T on the scattering distribution for grazing incidence. Theoretical curves calculated from scalar theory (eq. (1), $I_{scatter}$) using an exponential autocorrelation funtion (λ = 100 Å, Θ_3 = 0, R_o = 1).

Fig. 4 Comparison of the scalar theory /13/ with the vector theory /14/ for different optical materials (σ = 30 Å, T = 1000 Å, λ = 100 Å, Θ_3 = 0).

Fig. 5 Measured scattering intensity distributions (divided by R_o (Θ_1) and normalized to the incident intensity I_o) in the plane of incidence (Θ_3 = 0) with a fit by scalar theory (solid curve). A summary of all fit parameters is given in table 1.

Fig. 6 Same as figure 5 for the "1 µm-polished" sample, which was the most thoroughly characterized sample. I_o is the incident intensity profile.

Fig. 7 Same as figure 5 but "15 µm-polished" sample.

Fig. 8 Same as figure 5 but 2000 Å thick "rough gold coating".

Fig. 9 Upper part: "fit" with gaussian autocorrelation function (same sample as in figure 6).
Lower part: fit with the vector theory (eq. (2)) with the same roughness parameters as used in figure 6.

Fig. 10 The optical factor of the vector theory Q (Θ_1, Θ_2) as a function of Θ_2 for different optical constants and different Θ_1 and λ values. Since $Q(\Theta_1, \Theta_2 = \Theta_1) = R_o(\Theta_1)$ we normalized the curves at $\Theta_2 = \Theta_1$ to 1. The influence of the Q-factor as shown here for Θ_1 = 80° and λ = 100 Å on the theoretical scattering distribution (eq. (2)) is shown in fig. 4.

Fig. 11 Comparison between measurements of coated and uncoated polished samples, which were prepared as similar as possible. The different optical constants of glass and gold cause characteristic changes of the scattering intensity. Despite these changes the overall shape of the distributions from the coated samples closely follow those of the substrate, which confirms that a thin coating (500 Å Au) does not change the substrate roughness.

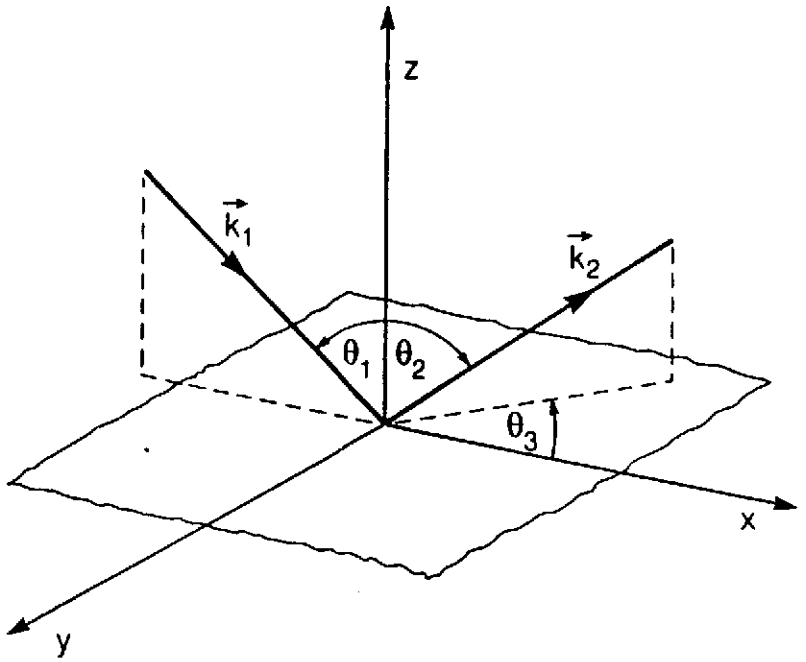

XBL 867-9855

Fig. 1

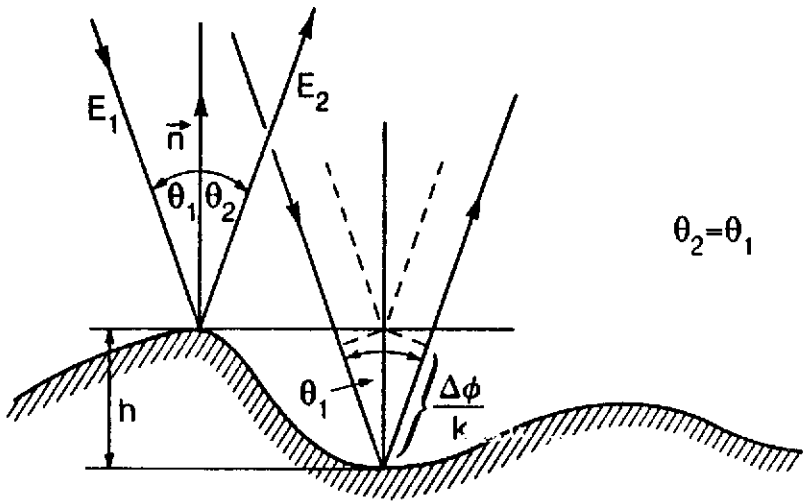

XBL 867-9856

Fig. 2

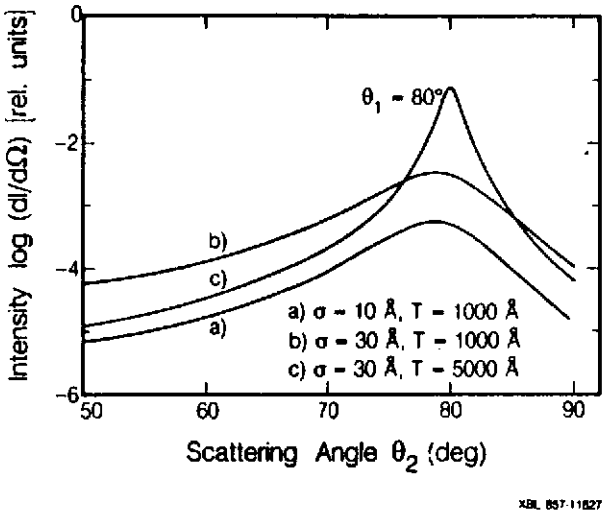

XBL 857-11827

Fig. 3

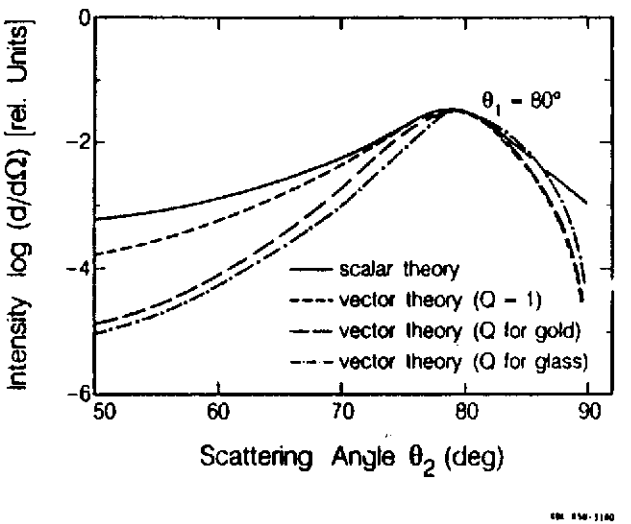

Fig. 4

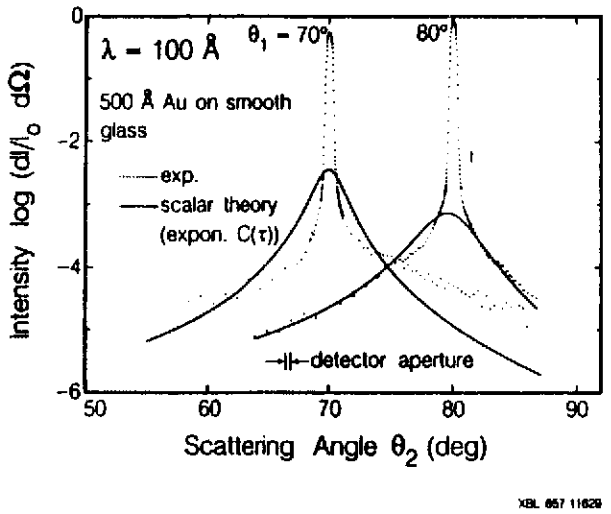
λ = 100 Å
θ1 = 70°
80°
500 Å Au on smooth glass
exp.
scalar theory (expon. C(τ))
detector aperture
Intensity log (dI/I0 dΩ)
Scattering Angle θ2 (deg)
XBL 857 11629

Fig. 5

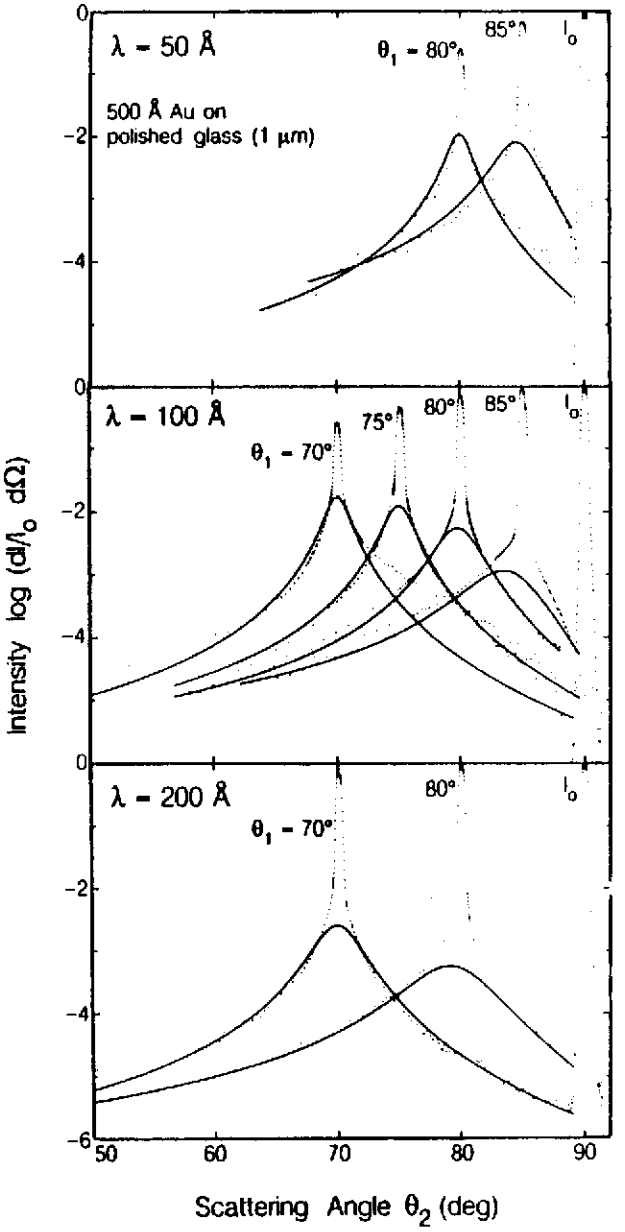
λ = 50 Å
θ1 = 80°
85°
I0
500 Å Au on polished glass (1 μm)
λ = 100 Å
θ1 = 70°
75°
80°
85°
I0
λ = 200 Å
θ1 = 70°
80°
I0
Intensity log (dI/I0 dΩ)
Scattering Angle θ2 (deg)
XBL 857-11635

Fig. 6

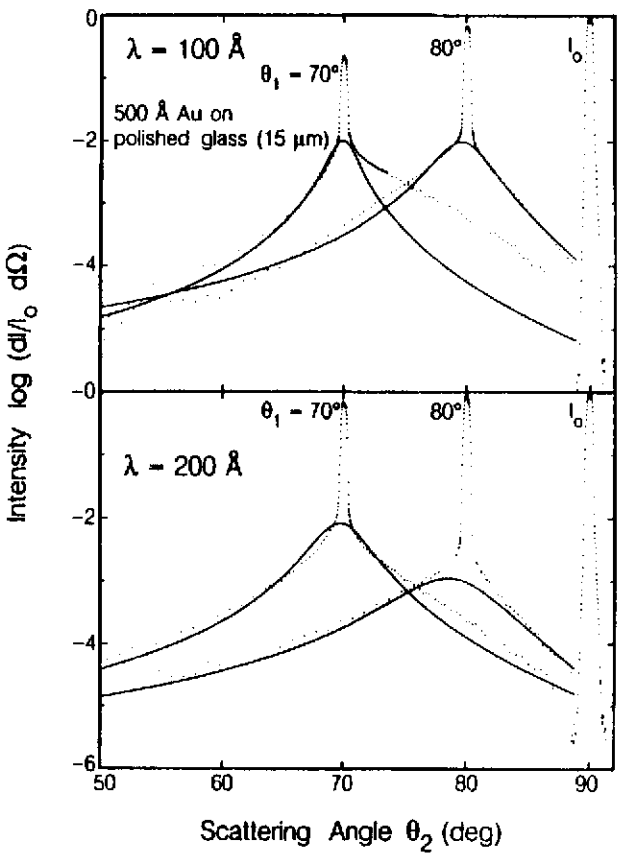

XBL 857 11630

Fig. 7

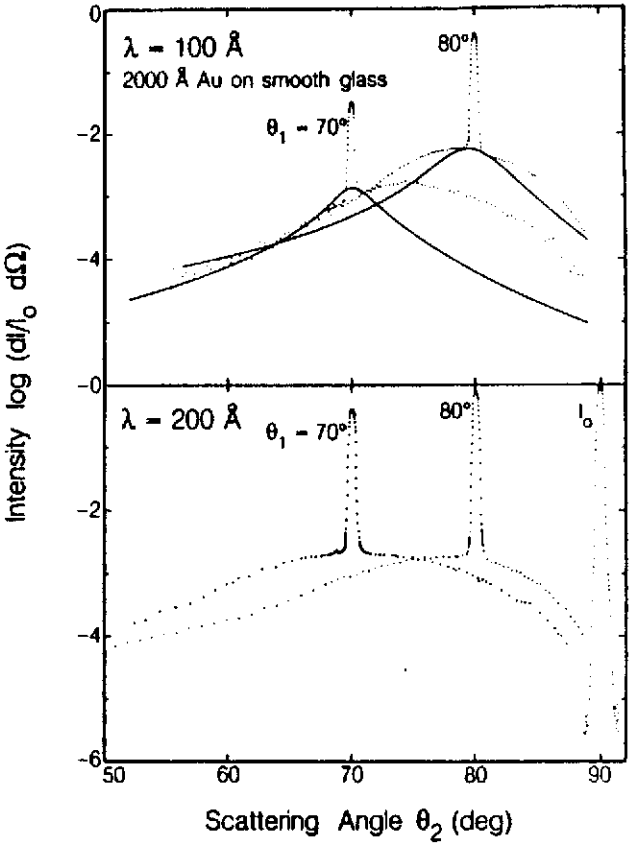

XBL 857 11633

Fig. 8

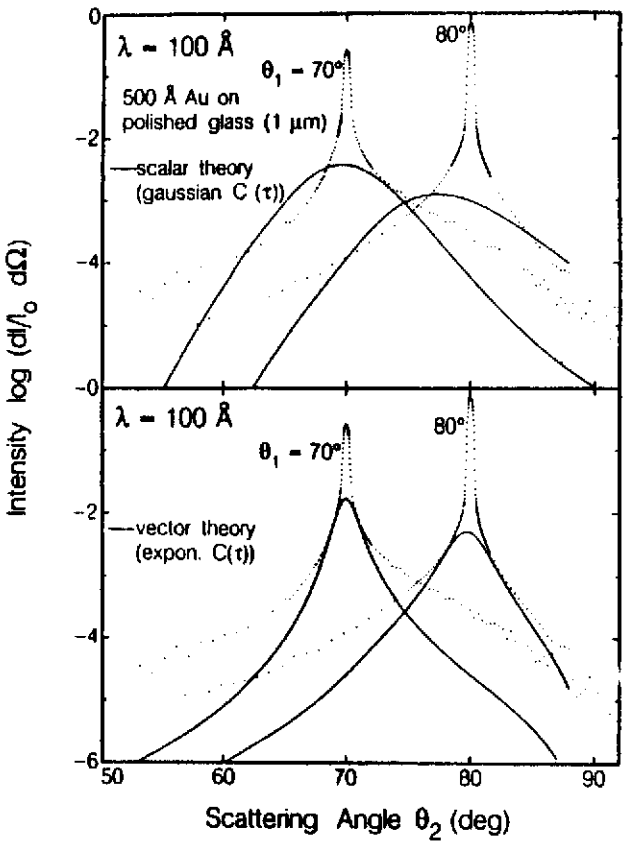

XBL 857-11631

Fig. 9

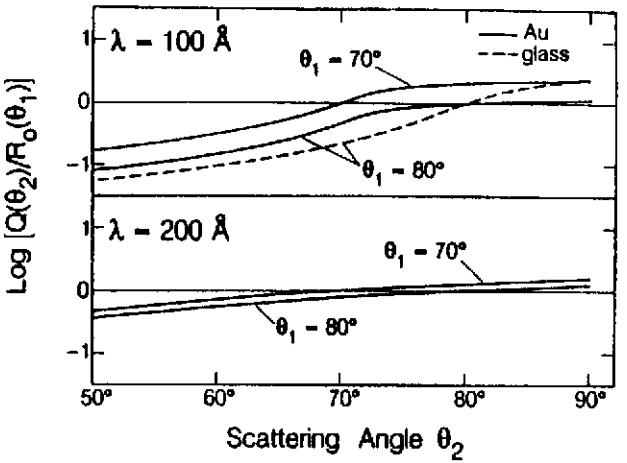

Fig. 10

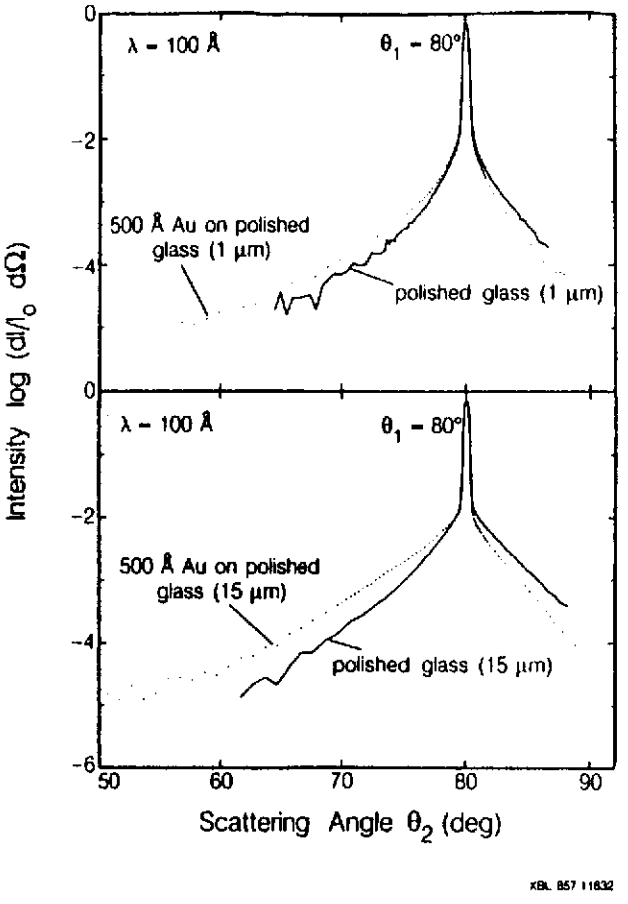

XBL 857 11632

Fig. 11